used to exclude any effect of obesity. When the CAD group was divided into uAP and sCAD subgroups, the preβ1-HDL level was markedly higher in the uAP subgroup than in the sCAD subgroup. Moreover, the difference remained significant even when dyslipidemic patients were excluded from the two subgroups (Table 2). The age, BMI, blood pressure and concentrations of HbA1c, hepatic function markers, renal function markers, HDL-C and apoA-I did not differ significantly between the two subgroups, although T-Cho, LDL-C and apoB were somewhat lower in the uAP subgroup than in the sCAD subgroup (Table 3). ROC analyses were performed to investigate the potential of preβ1-HDL as a predictive marker for uAP. Preβ1-HDL showed better diagnostic accuracy than other lipid markers, suggesting that preβ1-HDL may be useful for identifying patients with uAP (Fig. 1).

Two earlier studies reported elevation of the preβ1-HDL levels in CAD patients [16,17]. However, the mechanism responsible for that elevation has not been elucidated. Miida et al. reported that delayed catabolism of preβ1-HDL, specifically, delayed LCAT-dependent conversion of preβ1-HDL into α-migrating HDL, causes elevation of the preβ1-HDL level in CAD patients. However, they also described that some CAD patients had a high preβ1-HDL level despite the high LCAT activity, suggesting that some other mechanism may be responsible for preβ1-HDL elevation [16]. Asztalos et al. reported that CAD patients with low HDL-C levels (≤35 mg/dL) have high preβ1-HDL levels and suggested that delayed catabolism of preβ1-HDL is responsible for the elevated preβ1-HDL [17]. In our study, the normolipidemic CAD patients, excluding those with low HDL-C levels (<40 mg/dL), also showed elevated preβ1-HDL levels (Table 2). We speculate that the many uAP patients included in the present study may have been the cause of the elevated preβ1-HDL level in CAD patients without dyslipidemia. If, as has been suggested [17], delayed catabolism of preβ1-HDL is responsible for preβ1-HDL elevation, the HDL-C concentration and LCAT activity should be lower in the uAP subgroup than in the sCAD subgroup and should correlate negatively with the preβ1-HDL concentration. However, we could not find any difference in either the HDL-C concentration or the LCAT activity between the uAP and sCAD subgroups (Table 3), and there was no negative correlation between the preβ1-HDL concentration and either the HDL-C concentration or the LCAT activity in the CAD patients. In fact, the preβ1-HDL concentration conversely showed a significant and positive correlation with the HDL-C concentration in the CAD patients (Table 4 and Fig. 2A). In addition, the CAD patients with either a high HDL-C level or high LCAT activity also showed an elevated preβ1-HDL level (Table 2). These results suggest that some other mechanism must be responsible for preβ1-HDL elevation.

Perhaps that mechanism is enhancement of preβ1-HDL formation. The following three formation pathways are known: synthesis in the liver [9,10], new formation through interaction of apoA-I and peripheral cells [6–8] and dissociation through remodeling of α-HDL [11]. In the case of CAD, the last two of these preβ1-HDL formation pathways seem most likely and are discussed below.

Preβ1-HDL formation is increased in atherosclerotic CAD due to accelerated interaction of apoA-I and peripheral cells. It was reported that foam cell formation enhanced expression of ATP-binding cassette transporter A1 and apoA-I-mediated cholesterol efflux from cells in *in vitro* experiments [23,24]. Since preβ1-HDL is formed by the cellular cholesterol efflux of lipid-free apoA-I or lipid-poor apoA-I mediated by ABCA1 [3,4,6–8], the formation of preβ1-HDL in atherosclerotic CAD caused by accumulation of excess cholesterol might be accelerated by enhancement of that efflux in the peripheral cells.

The other most likely pathway of preβ1-HDL formation in uAP is that preβ1-HDL generation is enhanced by α-HDL remodeling caused by an increase in acute-phase proteins during inflammation. Serum amyloid A (SAA), group IIa secretory phospholipase A2 (sPLA2-IIa) and phospholipid transfer protein (PLTP), whose blood concentrations or activities are elevated in the acute-phase, are known to be factors that facilitate α-HDL remodeling [25–28]. For example, it was reported that the amount of SAA in HDL particles increases markedly during the acute inflammatory phase [28] and that it dissociates preβ1-HDL from α-HDL when it binds to α-HDL [29]. The blood concentration of SAA increases in uAP [30], and SAA is highly expressed in atherosclerotic lesions [31]. van der Westhuyzen et al. suggested a model for the acute-phase response in CAD in which SAA and sPLA2-IIa, present at sites of inflammation and tissue damage, play protective roles by enhancing cellular cholesterol efflux, thereby promoting the removal of excess cholesterol from macrophages [25]. Thus, acute-phase proteins, including SAA, seem to be factors promoting preβ1-HDL elevation in uAP, although the results of the present study are not sufficient to prove this hypothesis.

In summary, we demonstrated that the preβ1-HDL level is elevated in CAD patients, especially in uAP patients, even when excluding dyslipidemic subjects. These results suggest that elevation of the plasma preβ1-HDL level is associated with the atherosclerotic phase of CAD. Elevation of plasma preβ1-HDL may be useful for the identification of patients with uAP. Moreover, that elevation may be caused by a different mechanism from the previously proposed delayed catabolism of preβ1-HDL due to low LCAT activity.

Acknowledgement

We wish to thank Isao Nishina of Chiba Cardiovascular Center for his fine technical assistance.

References

[1] Castro GR, Fielding CJ. Early incorporation of cell-derived cholesterol into pre-β-migrating high-density lipoprotein. Biochemistry 1988;27:25–9.
[2] Barrans A, Jaspard B, Barbaras R, et al. Pre-β HDL: structure and metabolism. Biochim Biophys Acta 1996;1300:73–85.
[3] Fielding CJ, Fielding PE. Molecular physiology of reverse cholesterol transport. J Lipid Res 1995;36:211–28.
[4] Sviridov D, Nestel P. Dynamics of reverse cholesterol transport: protection against atherosclerosis. Atherosclerosis 2002;161:245–54.
[5] Yokoyama S. Apolipoprotein-mediated cellular cholesterol efflux. Biochim Biophys Acta 1998;1392:1–15.
[6] Okuhira K, Tsujita M, Yamauchi Y, et al. Potential involvement of dissociated apoA-1 in the ABCA1-dependent cellular lipid release by HDL. J Lipid Res 2004;45:645–52.
[7] Fitzgerald ML, Morris AL, Chroni A, et al. ABCA1 and amphipathic apolipoproteins form high-affinity molecular complexes required for cholesterol efflux. J Lipid Res 2004;45:287–94.
[8] Chau P, Nakamura Y, Fielding CJ, et al. Mechanism of prebeta-HDL formation and activation. Biochemistry 2006;45:3981–7.
[9] Jones LA, Teramoto T, John DJ, et al. Characterization of lipoproteins produced by the perfused rhesus monkey liver. J Lipid Res 1984;25:319–35.
[10] Castle CK, Pape ME, Marotti KR, et al. Secretion of pre-beta-migrating apoA-I by cynomolgus monkey hepatocytes in culture. J Lipid Res 1991;32:439–47.
[11] Rye KA, Clay MA, Barter PJ. Remodeling of high density lipoproteins by plasma factors. Atherosclerosis 1999;145:227–38.
[12] Glomset JA. The lecithin:cholesterol acyltransferase reaction. J Lipid Res 1968;9:155–67.
[13] Francone OL, Gurakar A, Fielding C. Distribution and functions of lecithin:cholesterol acyltransferase and cholesteryl ester transfer protein in plasma lipoproteins. J Biol Chem 1989;264:7066–72.
[14] Nakamura Y, Kotite L, Gan Y, et al. Molecular mechanism of reverse cholesterol transport: reaction of pre-β-migrating high-density lipoprotein with plasma lecithin/cholesterol acyltransferase. Biochemistry 2004;43:14811–20.
[15] Miyazaki O, Kobayashi J, Fukamachi I, et al. A new sandwich enzyme immunoassay for measurement of plasma pre-β1-HDL levels. J Lipid Res 2000;41:2083–8.
[16] Miida T, Nakamura Y, Inano K, et al. Preβ1-high density lipoprotein increases in coronary artery disease. Clin Chem 1996;42:1992–5.
[17] Asztalos BF, Roheim PS, Milani RL, et al. Distribution of apoA-I-containing HDL subpopulations in patients with coronary heart disease. Arterioscler Thromb Vasc Biol 2000;20:2670–6.

[18] Miida T, Miyazaki O, Nakamura Y, et al. Analytical performance of a sandwich enzyme immunoassay for preβ1-HDL in stabilized plasma. J Lipid Res 2003;44:645–50.
[19] Nagasaki T, Akanuma Y. A new colorimetric method for the determination of plasma lecithin–cholesterol acyltransferase activity. Clin Chim Acta 1977;75:371–5.
[20] Hanley JA, McNeil BJ. A method of comparing the areas under receiver operating characteristic curves derived from the same cases. Radiology 1983;148:839–43.
[21] Sasahara T, Yamashita T, Sviridov D, et al. Altered properties of high density lipoprotein subfractions in obese subjects. J Lipid Res 1997;38:600–11.
[22] Miida T, Miyazaki O, Hanyu O, et al. LCAT-dependent conversion of preβ1-HDL into α-migrating HDL is severely delayed in hemodialysis patients. J Am Soc Nephrol 2003;14:732–8.
[23] Langmann TJ, Klucken M, Reil G, et al. Molecular cloning of the human ATP-binding cassette transport 1 (hABC1): evidence of sterol-dependent regulation in macrophages. Biochem Biophys Res Commun 1999;257:29–33.
[24] Lawn RM, Wade DP, Garbin MR, et al. The Tangier disease gene product ABC1 controls the cellular apolipoprotein-mediated lipid removal pathway. J Clin Invest 1999;104:R25–31.
[25] van der Westhuyzen DR, de Beer FC, Webb NR. HDL cholesterol transport during inflammation. Curr Opin Lipidol 2007;18:147–51.
[26] Tiege UJ, Maugeais C, Cain W, et al. Overexpression of secretory phospholipase A(2) causes rapid catabolism and altered tissue uptake of high density lipoprotein cholesteryl ester and apolipoprotein A-I. J Biol Chem 2000;275:10077–84.
[27] Pussinen PJ, Malle E, Metso J, et al. Acute-phase HDL in phospholipid transfer protein (PLTP)-mediated HDL conversion. Atherosclerosis 2001;155:297–305.
[28] Malle E, Steinmetz A, Raynes JG. Serum amyloid A (SAA): an acute phase protein and apolipoprotein. Atherosclerosis 1993;102:131–46.
[29] Miida T, Yamada T, Yamadera T, et al. Serum amyloid A protein generates preβ1 high-density lipoprotein from α-migrating high density lipoprotein. Biochemistry 1999;38:16958–62.
[30] Kosuge M, Ebina T, Ishikawa T, et al. Serum amyloid A is a better predictor of clinical outcomes than C-reactive protein in non-ST-segment elevation acute coronary syndromes. Circ J 2007;71:186–90.
[31] Meek RL, Urieli-Shoval S, Benditt EP. Expression of apolipoprotein serum amyloid A mRNA in human atherosclerotic lesions and cultured vascular cells: implications for serum amyloid A function. Proc Natl Acad Sci U S A 1994;91:3186–90.

Tenomodulin Is Highly Expressed in Adipose Tissue, Increased in Obesity, and Down-Regulated during Diet-Induced Weight Loss

Atsuhito Saiki*, Maja Olsson*, Margareta Jernås, Anders Gummesson, Philip G. McTernan, Johanna Andersson, Peter Jacobson, Kajsa Sjöholm, Bob Olsson, Shigeo Yamamura, Andrew Walley, Philippe Froguel, Björn Carlsson, Lars Sjöström, Per-Arne Svensson, and Lena M. S. Carlsson

Sahlgrenska Center for Cardiovascular and Metabolic Research (A.S., M.O., M.J., A.G., J.A., P.J., K.S., B.O., B.C., L.S., P.-A.S., L.M.S.C.), Department of Molecular and Clinical Medicine, The Sahlgrenska Academy at Gothenburg University, 41345 Gothenburg, Sweden; Diabetes and Metabolism Unit (P.G.M.), Clinical Sciences Research Institute, Warwick Medical School, University of Warwick, University Hospital Coventry and Warwickshire, Coventry CV2 2DX, United Kingdom; Faculty of Pharmaceutical Sciences (S.Y.), Josai International University, 285-8555 Chiba, Japan; Section of Genomic Medicine (J.A., A.W., P.F.), Imperial College London, Hammersmith Hospital, London W12 0NN, United Kingdom; Centre National de la Recherche Scientifique-8090, Institute of Biology (P.F.), Pasteur Institute, 59019 Lille, France; and Department of Discovery Medicine (B.C.), AstraZeneca R&D, SE-431 83 Mölndal, Sweden

Context: Tenomodulin (TNMD), a putative angiogenesis inhibitor, is expressed in hypovascular connective tissues. Global gene expression scans show that the TNMD gene also is expressed in human adipose tissue and that its expression is regulated in response to weight reduction; however, more detailed information is lacking.

Objective: The aim of this study was to investigate TNMD tissue distribution and TNMD gene expression in human adipose tissue in relation to obesity and metabolic disease.

Design, Patients, and Interventions: TNMD gene expression, tissue distribution, and TNMD gene expression in adipose tissue from different depots, from lean and obese subjects, and during diet-induced weight reduction were analyzed by DNA microarray and real-time PCR.

Main Outcome Measure: We primarily measured TNMD gene expression.

Results: The TNMD gene was predominantly expressed in sc adipose tissue. TNMD gene expression was higher in sc than omental adipose tissue both in lean ($P = 0.002$) and obese subjects ($P = 0.014$). In both women and men, TNMD gene expression was significantly higher in the obese subjects compared to the lean subjects ($P = 1.1 \times 10^{-26}$ and $P = 0.010$, respectively). In a multiple linear regression analysis, BMI was a significant independent predictor of TNMD gene expression. TNMD gene expression was down-regulated during diet-induced weight loss, with a 65% decrease after 18 wk of diet ($P < 0.0001$).

Conclusions: We conclude that human adipose tissue TNMD gene expression is highly affected by obesity, adipose tissue location, and weight loss, indicating that TNMD may play a role in adipose tissue function. **(*J Clin Endocrinol Metab* 94: 3987–3994, 2009)**

ISSN Print 0021-972X ISSN Online 1945-7197
Printed in U.S.A.

doi: 10.1210/jc.2009-0292 Received February 9, 2009. Accepted July 2, 2009.
First Published Online July 14, 2009
*A.S. and M.O. are equal first authors of this study.

Abbreviations: BMI, Body mass index; BP, blood pressure; FFM, fat-free mass; FM, fat mass; HOMA-IR, homeostasis model assessment of insulin resistance; hs-CRP, highly sensitive C-reactive protein; PPIA, peptidyl-prolyl isomerase A; SVF, stromal vascular fraction; TNMD, tenomodulin; VLCD, very low calorie diet; WHR, waist to hip ratio.

Tenomodulin (TNMD), a protein consisting of 317 amino acids, is a member of a new family of type II transmembrane proteins. The human TNMD gene spans approximately 15 kb and is mapped to Xq22. TNMD is a putative angiogenesis inhibitor and is highly expressed in hypovascular connective tissues such as tendons and cartilage (1–4). Studies of global gene expression show that the TNMD gene is also expressed in human adipose tissue. In two DNA microarray screens (5, 6), the TNMD gene was among the genes that were down-regulated in response to weight reduction, and in one of the studies TNMD gene expression was correlated with insulin sensitivity (5). The link between TNMD and metabolic disease is further highlighted by studies showing that TNMD polymorphisms are associated with obesity, diabetes risk (7), systemic immune mediators (8), and cholesterol levels (9). However, the mechanisms behind these associations are unknown.

Together, these findings suggest that TNMD could have metabolic effects in addition to its role in angiogenesis. However, more detailed information on the regulation of TNMD gene expression in human tissues is lacking. For example, the relative expression level of this gene in adipose tissue in relation to other human tissues needs to be established, and it is unknown whether there are differences in TNMD gene expression between lean and obese subjects. The aim of this study was therefore to determine the tissue distribution of TNMD gene expression and to investigate the expression of TNMD gene in adipose tissue in relation to obesity, weight loss, and metabolic risk factors in large and well-characterized cohorts to gain insights into the possible role of TNMD in human obesity and obesity comorbidities.

Subjects and Methods

All study subjects received written and oral information before giving written informed consent. The Regional Ethics Committee in Gothenburg and the South Birmingham Ethics Committee approved these studies. Patient characteristics are described as mean ± SD in Table 1.

The depot study

Women undergoing elective surgery (liposuction and elective gynecological procedures) were recruited, and paired abdominal sc and abdominal omental (n = 10) adipose tissue biopsies were collected in accordance with guidelines of the South Birmingham Ethics Committee. Smokers and subjects with recent weight change, hormone replacement, and malignant diseases were excluded. The subjects were divided into two cohorts (Table 1) according to BMI (lean, n = 5; BMI, 23.0 ± 1.2 kg/m^2; obese, n = 5; BMI, 33.2 ± 3.1 kg/m^2).

The Swedish Obese Subjects (SOS) Sib Pair study

The SOS Sib Pair study consists of 154 nuclear families with BMI discordant sibling pairs (BMI difference ≥ 10 kg/m^2), resulting in a study population consisting of 732 subjects. In the current study, the most extreme siblings according to BMI were chosen in each family, and gender discordant sibling pairs were excluded, resulting in 78 pairs of sisters and 12 pairs of brothers with one of the siblings classified as obese and the other sibling classified as lean (Table 1) (10, 11).

Diet-induced weight loss (VLCD) studies

The very low calorie diet (VLCD) study was performed to identify gene expression changes in adipose tissue of obese subjects during weight loss by caloric restriction (12–15). Forty obese (BMI > 30 kg/m^2) subjects were included in the study, of which 24 subjects (18 males and six females) were analyzed by DNA microarray (Table 1). At the start of the study, the 24 subjects were divided into two groups, one group with the metabolic syndrome (n = 12) and one group without the metabolic syndrome (n = 12) (12, 16). All subjects were treated with a VLCD (450 kcal/d) for 16 wk, followed by 2 wk when regular food was gradually reintroduced. Study assessments were performed at the start of VLCD treatment (wk 0), twice during the VLCD phase (wk 8 and 16), and 2 wk after the end of VLCD treatment (wk 18) when regular food gradually had been reintroduced.

An additional 28 obese subjects (BMI > 30 kg/m^2) subjects (eight males and 20 females) were included for the verification of TNMD expression during VLCD. The subjects were treated with VLCD for 12 wk. Study assessments were performed at the start of VLCD treatment (wk 0) and three times during the VLCD phase (wk 2, 6, and 12). The mean weight loss after 12 wk of VLCD was 19%. TNMD expression was analyzed using real-time PCR as described below.

TABLE 1. Characteristics of the subjects and samples used in this study

	Sib Pair study		VLCD (microarray)	VLCD (real-time PCR)	Depot study	
	Lean	Obese	Obese	Obese	Lean	Obese
n	90	90	24	28	5	5
Sex (M/F)	12/78	12/78	18/6	8/20	0/5	0/5
Age (yr)	36.3 ± 7.5	39.3 ± 6.5	48.3 ± 10.2	39.7 ± 12.7	40 ± 7	50 ± 4
BMI (kg/m^2)	22.0 ± 1.7	37.7 ± 5.3	37.6 ± 4.9	36.3 ± 3.7	23.0 ± 1.2	33.2 ± 3.1
AT depot	sc	sc	sc	sc	sc, om	sc, om
Biopsy procedure	Needle	Needle	Needle	Needle	Surgical	Surgical

Values are presented as mean ± SD. AT, Adipose tissue; om, omental.

Tissue distribution of TNMD gene expression

To determine the tissue distribution of TNMD gene expression, DNA microarray expression profiles of 65 human tissues were acquired from the Gene Expression Omnibus (GEO) database (Dataset GSE3526; http://www.ncbi.nlm.nih.gov/geo/). Each tissue in this data set is represented by Human Genome U133 plus 2.0 DNA microarray expression profiles (Affymetrix, Santa Clara, CA) from three to nine different individuals. TNMD gene expression was investigated using the 220065_at probe set.

Adipose tissue biopsies and RNA preparation

Abdominal sc adipose tissue biopsies obtained by needle aspirations or surgical adipose tissue biopsies (Table 1) were flash frozen and stored at −80 C until analysis. For analysis of tissue distribution, adipocytes were isolated from fresh adipose tissue biopsies as previously described (17, 18). Total RNA was prepared with the RNeasy lipid tissue kit (QIAGEN, Chatsworth, CA), or using the phenol-chloroform extraction method of Chomczynski and Sacchi (19) with further purification with RNeasy clean-up columns. The RNA concentration was measured spectrophotometrically, and the A260/A280 ratio was 1.8–2.0. The quality of the RNA was verified by agarose gel electrophoresis before reverse transcription into cDNA.

DNA microarray analysis

Gene expression in paired abdominal sc and omental adipose tissue samples from the depot study and samples from the SOS Sib Pair study were analyzed using the Human Genome U133 plus 2.0 DNA microarrays (Affymetrix). In the VLCD study, gene expression was analyzed using the Human Genome U133A DNA microarray (Affymetrix). Preparation of cDNA and hybridization to DNA microarray was performed according to standard Affymetrix protocols. The hybridization and analysis were performed according to the Minimum Information about a Microarray Experiment guideline (20). Gene expression profiles from the adipose tissue samples were analyzed using the RMA software (Affymetrix). TNMD gene expression was investigated using the 220065_at probe set.

Adipocyte and stromal vascular fraction cells isolation

For verification of tissue distribution, total RNA was prepared with RNeasy Lipid Tissue Mini Kit (QIAGEN) from sc adipose tissue, and isolated sc adipocytes from healthy volunteers (two females, one male with BMI of 22.4–26.7 kg/m^2; and two females, one male with BMI of 22.4–29.3 kg/m^2, respectively).

Subcutaneous adipose tissue needle biopsies for the preparation of stromal vascular fraction (SVF) cells were obtained from three subjects. In brief, the adipose tissue was minced, collagenase was digested, and the digested adipose tissue was then filtered through a 250-μm mesh net. Nonbuoyant liberated cells were collected by centrifugation. TNMD expression in SVF cells was compared with the expression levels in sc adipose tissue from eight subjects (two males and six females) using real-time PCR.

Real-time PCR analysis

RNA from adipose tissue, adipocytes, SVF cells, and RNA from the Human Total RNA Master Panel II (Clontech Laboratories, Inc., Palo Alto, CA), were reversed transcribed using the High Capacity cDNA RT kit (Applied Biosystems, Foster City, CA) according to the manufacturer's protocol. Reagents for real-time PCR analysis of TNMD (Hs00223332_m1), low-density lipoprotein (LDL) receptor-related protein 10 (LPR10) (Hs00204094_m1), and peptidyl-prolyl isomerase A (PPIA) (Hs99999904_m1) (Assays-on-Demand and TaqMan Universal PCR Master mix) were purchased from Applied Biosystems and used according to the manufacturer's protocol. cDNA corresponding to 10 ng RNA per reaction was used for real-time PCR in the ABI PRISM 7900HT Sequence Detection System (Applied Biosystems). A standard curve was plotted for each primer-probe set with a serial dilution of cDNA synthesized from pooled RNA. PPIA or LRP10 gene expression was used to normalize TNMD gene expression between samples. All samples and standards were analyzed in triplicate.

Measurements

In the SOS Sib Pair study, anthropometry and measurements of fat mass (FM), fat-free mass (FFM), blood pressure (BP), fasting glucose, total cholesterol, triglyceride, high-density lipoprotein (HDL) cholesterol, LDL cholesterol, serum insulin, serum C-peptide, highly sensitive C-reactive protein (hs-CRP), and homeostasis model assessment of insulin resistance (HOMA-IR) were performed at the Sahlgrenska University Hospital. Body composition assessed by dual-energy x-ray absorptiometry was performed with LUNAR DPX-L (Scanexport Medical, Helsingborg, Sweden). The dual-energy x-ray absorptiometry examination generates a three-compartment model consisting of FM, lean tissue mass (LTM), and bone mineral content (BMC). The FFM was calculated as LTM + BMC. All measurements and samplings were performed after an overnight fast.

Statistics

Values are given as mean ± SEM unless otherwise indicated. To obtain approximate normal distributions of expression data, DNA microarray signals in the whole SOS Sib Pair study offspring cohort (n = 359) were transformed using Box-Cox power transformations. Subsequently, expression data were standardized to mean = 0 and variance = 1. Differences in TNMD gene expression between lean and obese siblings were assessed using paired t test. In the SOS Sib Pair study, Spearman rank correlation analysis between TNMD gene expression and clinical parameters was performed. In addition, multiple linear regression analysis was used to evaluate independent associations. In the multiple linear regression analysis, the dependent variable was TNMD gene expression, and the independent variables were BMI, diastolic BP, triglyceride, C-peptide, hs-CRP, and HOMA-IR. The independent variables—waist, waist to hip ratio (WHR), FM, FFM, systolic BP, fasting glucose, total cholesterol, HDL cholesterol, LDL cholesterol, and insulin—were excluded from the model due to multicollinearity. In the VLCD studies, paired t test was used to test differences in TNMD gene expression between time points, and Student's t test was used to assess differences in TNMD gene expression between subjects with and without metabolic syndrome or sex differences at baseline. Differences in TNMD expression in paired abdominal sc and omental adipose tissue were tested using paired t test. Two-sided P values less than 0.05 were considered statistically significant.

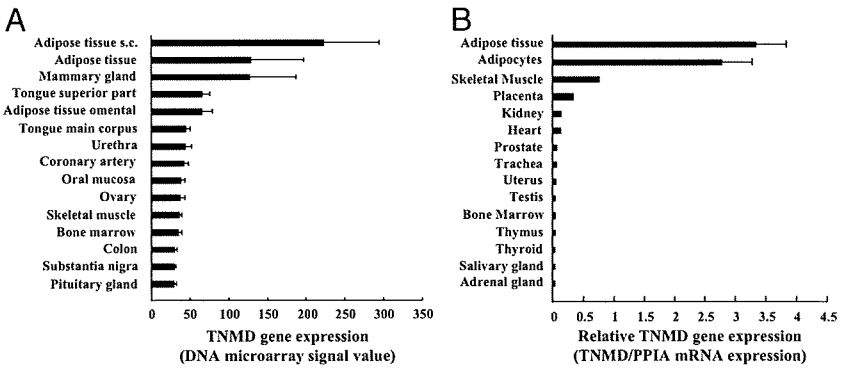

FIG. 1. Tissue distribution of TNMD gene expression. A, Results from DNA microarray analysis presenting the 15 tissues with the highest TNMD gene expression out of the 65 tissues that were compared. The data were obtained from the GEO database (GSE3526). B, Results from the validation of TNMD gene expression with real-time PCR in isolated adipocytes (n = 3), adipose tissue (n = 3), and a human tissue panel. The figure shows the 15 tissues with the highest TNMD gene expression out of the 20 tissues that were compared. Values are given as mean ± SEM.

Results

Expression of the TNMD gene in human adipose tissue and adipocytes

The tissue distribution of TNMD gene expression was initially investigated using publicly available DNA microarray expression profiles obtained from the GEO database (Fig. 1A). This analysis included 65 human tissues and showed that sc adipose tissue had the highest expression of the TNMD gene, followed by adipose tissue of undefined origin, mammary gland, and omental adipose tissue.

To investigate TNMD gene expression in adipocytes and to verify the tissue distribution of TNMD gene expression, real-time PCR analysis was performed on isolated sc adipocytes and sc adipose tissue and a panel of 18 other human tissues (Human Total RNA Master Panel II, Clontech Laboratories) (Fig. 1B). High TNMD gene expression levels were observed in adipocytes and adipose tissue. The expression of the TNMD gene was at least 3-fold higher in isolated adipocytes and adipose tissue compared with the other human tissues. TNMD expression in isolated SVF cells from sc adipose tissue (1.2 ± 0.4 TNMD/PPIA mRNA) was similar to that in whole sc adipose tissue (0.8 ± 0.2 TNMD/PPIA mRNA).

Regional differences in expression of TNMD gene in human adipose tissues

The DNA microarray analysis of tissue distribution indicated that sc adipose tissue displayed higher levels of TNMD gene expression compared with omental adipose tissue (Fig. 1A). We therefore measured TNMD gene expression by DNA microarray analysis in paired abdominal sc and omental adipose tissue samples (Fig. 2A) from the depot study (five lean and five obese subjects). TNMD gene expression was significantly higher in sc adipose tissue compared with omental adipose tissue both in lean ($P = 0.002$) and obese subjects ($P = 0.014$). Using real-time PCR, this depot difference was verified ($P = 0.014$) in the obese subjects (Fig. 2B), whereas there was no significant difference in the lean subjects.

Expression of TNMD gene in lean and obese subjects

TNMD gene expression in sc adipose tissue from BMI-discordant sibling pairs from the SOS Sib Pair study was measured by DNA microarray analysis. In both women and men, TNMD gene expression was significantly higher in the obese subjects compared with the lean subjects ($P = 1.1 \times 10^{-26}$ and $P = 0.010$, respectively) (Fig. 3). There was also an increased expression of TNMD in the obese women compared with the obese men ($P = 0.0044$), whereas there was no gender difference in the lean subjects.

We next investigated the relationship between adipose tissue TNMD gene expression and clinical parameters in the SOS Sib Pair study (Table 2). When all subjects were analyzed together, TNMD gene expression correlated with measures of obesity, adipose tissue distribution, BP, serum lipid levels, and markers of carbohydrate metabolism. When the lean and obese siblings were analyzed separately, TNMD gene expression correlated positively with BMI both in lean subjects ($P < 0.001$) and in obese subjects ($P = 0.001$) (Table 2). Positive correlations between TNMD gene expression and waist circumference, FM, serum triglyceride concentrations, serum C-peptide concentrations,

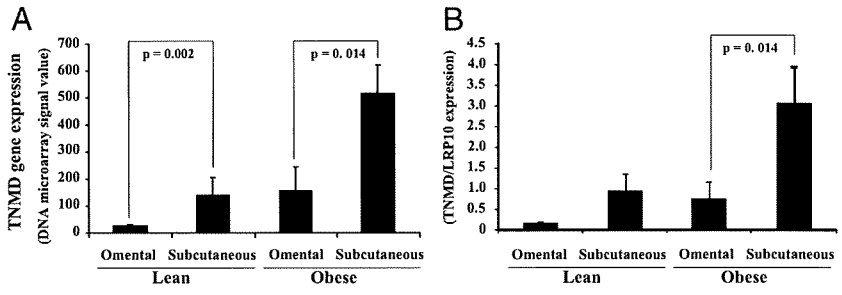

FIG. 2. Regional differences in adipose tissue expression of the TNMD gene. TNMD gene expression in paired abdominal sc and omental adipose tissue biopsies from the depot study was analyzed by DNA microarray (A) and real-time PCR (B). Values are given as mean ± SEM.

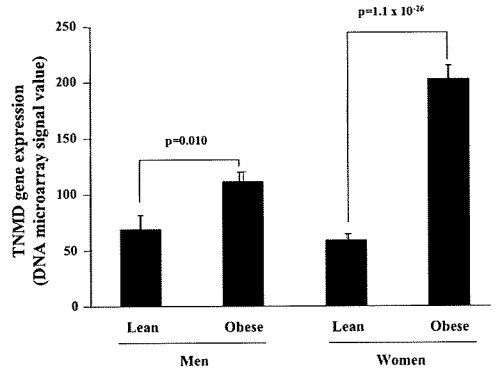

FIG. 3. TNMD gene expression in adipose tissue from BMI-discordant sibling pairs in the SOS Sib Pair study. RNA was isolated from sc adipose tissue biopsies from 90 sibling pairs (78 pairs of sisters and 12 pairs of brothers), and TNMD gene expression was analyzed by DNA microarray. Values are given as mean ± SEM.

and negative correlations with serum HDL cholesterol levels also persisted in both groups. Multiple linear regression analysis showed that BMI was a significant independent predictor for TNMD gene expression when all subjects were analyzed together. BMI was also a significant independent predictor for TNMD gene expression in the lean subjects group (Table 2).

Expression of TNMD gene during diet-induced weight loss

The high expression of TNMD gene in obese subjects and the correlations with metabolic risk factors led us to examine whether VLCD treatment, resulting in large weight losses and improved metabolic status (12), affected adipose tissue TNMD gene expression. Adipose tissue TNMD gene expression was markedly reduced after 8 wk of diet (29% decrease from wk 0) and after 16 wk of diet (48% decrease from wk 0) (Fig. 4A). Between wk 16 and 18, when regular food was gradually reintroduced, the average body weight was unchanged, and TNMD gene expression remained low (65% decrease from wk 0). No difference in TNMD gene expression was seen at baseline between the obese subjects with the metabolic syndrome and the obese subjects without metabolic syndrome. To

TABLE 2. Correlation coefficients between TNMD gene expression in adipose tissue and clinical parameters in Sib Pair study

Variables		Spearman rank correlation test (r)			Multiple linear regression (β-coefficient)		
		All	Lean	Obese	All	Lean	Obese
n		180	90	90	180	90	90
BMI (kg/m^2)	29.9 ± 8.8	0.758^c	0.398^c	0.355^b	0.081^c	0.125^a	0.038
Waist (cm)	95.4 ± 20.9	0.730^c	0.354^b	0.237^a			
WHR	0.87 ± 0.10	0.666^c	0.331^b	0.099			
FM (kg)	31.1 ± 16.0	0.708^c	0.209^a	0.295^a			
FFM (kg)	52.2 ± 9.5	0.465^c	0.021	0.102			
Systolic BP (mm Hg)	114.2 ± 15.7	0.403^c	0.182	0.047			
Diastolic BP (mm Hg)	69.6 ± 11.1	0.434^c	0.164	0.280^a	0.003	0.006	0.002
Total cholesterol (mmol/liter)	4.41 ± 0.83	0.125	−0.094	0.025			
Triglyceride (mmol/liter)	1.04 ± 0.76	0.546^c	0.233^a	0.343^b	0.197	0.130	0.131
HDL cholesterol (mmol/liter)	1.30 ± 0.35	−0.516^c	−0.389^c	−0.277^a			
LDL cholesterol (mmol/liter)	2.66 ± 0.64	0.231^b	0.052	−0.030			
Fasting glucose (mmol/liter)	4.94 ± 1.09	0.330^c	0.037	0.127			
Insulin (mU/liter)	9.67 ± 8.19	0.647^c	0.173	0.430^c			
HOMA-IR	2.23 ± 2.40	0.654^c	0.176	0.414^c	−0.023	0.131	0.005
C-peptide (mmol/liter)	0.71 ± 0.45	0.676^c	0.231^a	0.465^c	0.037	0.024	0.078
hs-CRP (mg/liter)	4.48 ± 6.88	0.578^c	0.208	0.251^a	0.001	0.012	−0.001

Values are expressed as mean ± SD. Correlation between TNMD gene expression and clinical parameters were performed using both the Spearman rank correlation test and the multiple linear regression analysis. In the multiple linear regression analysis, the dependent variable was TNMD gene expression, and the independent variables (waist, WHR, FM, FFM, systolic BP, fasting glucose, total cholesterol, HDL cholesterol, LDL cholesterol, and insulin) were excluded from the model due to multicollinearity.

^{a} $P < 0.05$.

^{b} $P < 0.005$.

^{c} $P < 0.001$.

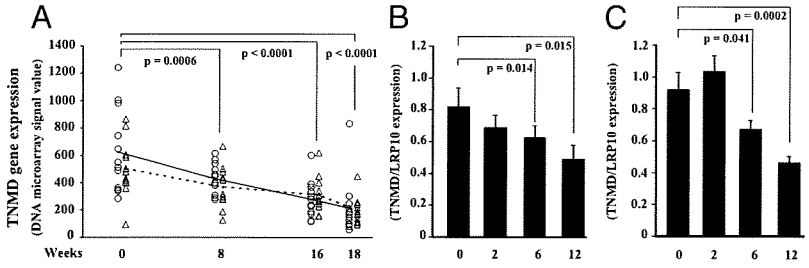

FIG. 4. Effect of diet-induced weight loss on adipose tissue TNMD gene expression. Twelve obese subjects with the metabolic syndrome (*solid lines and circles*) and 12 obese subjects without the metabolic syndrome (*dashed lines and triangles*) were treated with VLCD for 16 wk, followed by a 2-wk gradual reintroduction of regular food. Subcutaneous adipose tissue biopsies obtained at wk 0, 8, 16, and 18 and TNMD expression were analyzed by DNA microarray (A). Real-time PCR verification of the down-regulation of TNMD expression during diet-induced weight-loss was performed in eight males (B) and in 20 females (C). Subcutaneous adipose tissue biopsies obtained at wk 0, 2, 6, and 12 were used for the analysis. Values are given as mean ± SEM.

verify this finding, TNMD expression was analyzed in additional obese subjects receiving VLCD treatment for 12 wk. Significantly reduced TNMD expression was observed after 6 and 12 wk of VLCD treatment both in males (Fig. 4B) and in females (Fig. 4C). There was no gender difference in TNMD expression before the start of the VLCD treatment.

Discussion

Previously, TNMD has mainly been regarded as an inhibitor of angiogenesis in connective tissues, but this study shows that human adipose tissue is a major site of expression of the TNMD gene. TNMD expression in sc adipose tissue was markedly increased in obese compared with lean subjects, and BMI was an independent predictor of TNMD gene expression. We also show that TNMD gene expression was higher in sc compared with omental adipose tissue and that the expression in adipose tissue was down-regulated during weight loss.

Interestingly, TNMD polymorphisms have been associated with obesity, alterations in carbohydrate metabolism, and dyslipidemia (7, 9), but the mechanisms behind these associations are completely unknown. TNMD gene has previously been shown to be mainly expressed in tendons and cartilage (1–4); however, it is unlikely that TNMD production in these tissues explains the genetic associations to obesity and metabolic disorders. Although none of the tissue panels included human tendons or cartilage, our results clearly show that adipose tissue is a major site of TNMD gene expression and open the possibility that the genetic associations between TNMD and obesity and metabolism are related to TNMD effects in adipose tissue. We also found high expression of the TNMD gene in the mammary gland. However, in the tissue distribution dataset, high gene expression of adipocyte markers such as leptin and adiponectin was also observed in the mammary gland samples, strongly suggesting that the high TNMD gene expression was due to the presence of adipose tissue in the mammary gland biopsies. Our analysis also shows that both adipocytes and stromal vascular fraction cells contribute to TNMD expression in adipose tissue.

It has previously been shown that TNMD expression correlates with body FM in obese subjects (5), and in our study, adipose tissue TNMD gene expression was increased in obese compared with lean subjects. Together with the unexpectedly high expression in adipose tissue compared with other human tissues, this suggests that TNMD plays a role in adipocyte function. Our initial analysis of the relationship between adipose tissue TNMD expression and clinical traits showed that TNMD expression was closely linked to all the measured parameters, with the exception of total cholesterol levels. When this relationship was analyzed separately for the lean and obese subjects in the SOS Sib Pair study, the relationship between insulin levels and HOMA-IR and TNMD expression only existed in the obese subjects. However, many of these traits are intercorrelated, and multiple linear regression analysis in the SOS Sib Pair study showed that BMI was the only independent predictor of adipose tissue TNMD gene expression.

It is well established that weight loss results in amelioration of metabolic disturbances in the obese (12). Previous studies have shown that TNMD expression is reduced both immediately after diet-induced weight loss (5, 6) and during the weight-stable maintenance phase after diet-induced weight loss (5). Our VLCD study verifies and extends these findings by demonstrating that TNMD gene expression was reduced during the hypocaloric diet (wk 8 and 16) and remained low during the weight-stable period when ordinary food had been reintroduced. Thus, available information indicates that it is the reduction in body weight, rather than the caloric restriction, that reduces TNMD expression. In addition, our observation that BMI was an independent predictor of TNMD gene expression in the SOS Sib Pair study strengthens this view.

The TNMD gene is located on the X chromosome, and gender differences in adipose tissue TNMD expression have been reported in obese subjects both before and after weight-loss intervention (5). In the SOS Sib Pair study, this gender difference was only observed in the obese subjects, and not in the lean subjects. Characterization of the TNMD promoter and transcription factors controlling

TNMD expression might give insights into the mechanisms driving this BMI-dependent gender difference.

Our human data suggest that there is a tight association between adipose tissue TNMD gene expression and obesity; however, the situation may be different in rodents. TNMD-deficient mice have reduced tenocyte proliferation and tenocyte density but no change in size or weight compared with wild-type control mice (1), potentially arguing against a role for TNMD in obesity and metabolic disease. However, database searches indicate that mice, in marked contrast to humans, do not express the TNMD gene in adipose tissue (http://symatlas.gnf.org/SymAtlas/; gnf1m04203_a_at), suggesting that the function of TNMD in mice and man may differ.

TNMD has mainly been investigated as an inhibitor of angiogenesis. It is not known whether TNMD inhibits angiogenesis in adipose tissue. The idea that it may influence blood vessel development is intriguing because angiogenesis has recently been suggested to play a role in adipose tissue growth (21–23); however, functional studies are needed to address this question.

In conclusion, the TNMD gene is highly expressed in human adipose tissue. The increased expression of the TNMD gene in adipose tissue of obese subjects together with the down-regulation in response to weight loss lends support to the idea that TNMD plays a role in human adipose tissue function.

Acknowledgments

We acknowledge Dr. Jenny Palming for help with SVF cell preparation.

Address all correspondence and requests for reprints to: Dr. Per-Arne Svensson, Sahlgrenska Center for Cardiovascular and Metabolic Research, Department of Molecular and Clinical Medicine, The Sahlgrenska Academy at Gothenburg University, Vita Stråket 15, 413 45 Gothenburg, Sweden. E-mail: per-arne.svensson@medic.gu.se.

This work was supported by grants from the Swedish Research Council (K2007-55X-11285-13-3, K2008-65x-20753-01-4, 529-2002-6671), the Swedish Foundation for Strategic Research to Sahlgrenska Center for Cardiovascular and Metabolic Research, the Swedish Diabetes Foundation, the Dr. P. Håkanssons Foundation, the Åke Wiberg Foundation, the Foundations of the National Board of Health and Welfare, the Jeansson Foundations, the Magn Bergvall Foundation, the Tore Nilsson Foundation for Medical Research, the Royal Physiographic Society (Nilsson-Ehle Foundation), VINNOVA-VINNMER, the Swedish Knowledge Foundation through the Industrial Ph.D. program in Medical Bioinformatics at Corporate Alliances at Karolinska Institutet, the Swedish federal government under the LUA/ALF agreement, and The Wellcome Trust (GR079534).

Disclosure Summary: B.C. is employed by AstraZeneca. The other authors have nothing to disclose.

References

1. Docheva D, Hunziker EB, Fässler R, Brandau O 2005 Tenomodulin is necessary for tenocyte proliferation and tendon maturation. Mol Cell Biol 25:699–705
2. Brandau O, Meindl A, Fässler R, Aszódi A 2001 A novel gene, tendin, is strongly expressed in tendons and ligaments and shows high homology with chondromodulin-I. Dev Dyn 221:72–80
3. Shukunami C, Oshima Y, Hiraki Y 2001 Molecular cloning of tenomodulin, a novel chondromodulin-I related gene. Biochem Biophys Res Commun 280:1323–1327
4. Yamana K, Wada H, Takahashi Y, Sato H, Kasahara Y, Kiyoki M 2001 Molecular cloning and characterization of CHM1L, a novel membrane molecule similar to chondromodulin-I. Biochem Biophys Res Commun 280:1101–1106
5. Kolehmainen M, Salopuro T, Schwab US, Kekäläinen J, Kallio P, Laaksonen DE, Pulkkinen L, Lindi VI, Sivenius K, Mager U, Siitonen N, Niskanen L, Gylling H, Rauramaa R, Uusitupa M 2008 Weight reduction modulates expression of genes involved in extracellular matrix and cell death: the GENOBIN study. Int J Obes (Lond) 32:292–303
6. Dahlman I, Linder K, Arvidsson Nordström E, Andersson I, Lidén J, Verdich C, Sørensen TI, Arner P 2005 Changes in adipose tissue gene expression with energy-restricted diets in obese women. Am J Clin Nutr 81:1275–1285
7. Tolppanen AM, Pulkkinen L, Kolehmainen M, Schwab U, Lindström J, Tuomilehto J, Uusitupa M 2007 Tenomodulin is associated with obesity and diabetes risk: the Finnish diabetes prevention study. Obesity (Silver Spring) 15:1082–1088
8. Tolppanen AM, Pulkkinen L, Herder C, Koenig W, Kolehmainen M, Lindström J, Tuomilehto J, Uusitupa M 2008 The genetic variation of the tenomodulin gene (TNMD) is associated with serum levels of systemic immune mediators—the Finnish Diabetes Prevention Study. Genet Med 10:536–544
9. Tolppanen AM, Pulkkinen L, Kuulasmaa T, Kolehmainen M, Schwab U, Lindström J, Tuomilehto J, Uusitupa M, Kuusisto J 2008 The genetic variation in the tenomodulin gene is associated with serum total and LDL cholesterol in a body size-dependent manner. Int J Obes (Lond) 32:1868–1872
10. Carlsson LM, Jacobson P, Walley A, Froguel P, Sjöström L, Svensson PA, Sjöholm K 2009 ALK7 expression is specific for adipose tissue, reduced in obesity and correlates to factors implicated in metabolic disease. Biochem Biophys Res Commun 382:309–314
11. Jernås M, Olsson B, Arner P, Jacobson P, Sjöström L, Walley A, Froguel P, McTernan PG, Hoffstedt J, Carlsson LM 2009 Regulation of carboxylesterase 1 (CES1) in human adipose tissue. Biochem Biophys Res Commun 383:63–67
12. Gummesson A, Jernås M, Svensson PA, Larsson I, Glad CA, Schéle E, Gripeteg L, Sjöholm K, Lystig TC, Sjöström L, Carlsson B, Fagerberg B, Carlsson LM 2007 Relations of adipose tissue CIDEA gene expression to basal metabolic rate, energy restriction, and obesity: population-based and dietary intervention studies. J Clin Endocrinol Metab 92:4759–4765
13. Palming J, Sjöholm K, Jernås M, Lystig TC, Gummesson A, Romeo S, Lönn L, Lönn M, Carlsson B, Carlsson LM 2007 The expression of NAD(P)H:quinone oxidoreductase 1 is high in human adipose tissue, reduced by weight loss, and correlates with adiposity, insulin sensitivity, and markers of liver dysfunction. J Clin Endocrinol Metab 92:2346–2352
14. Sjöholm K, Palming J, Olofsson LE, Gummesson A, Svensson PA, Lystig TC, Jennische E, Brandberg J, Torgerson JS, Carlsson B, Carlsson LM 2005 A microarray search for genes predominantly expressed in human omental adipocytes: adipose tissue as a major production site of serum amyloid A. J Clin Endocrinol Metab 90:2233–2239
15. Sjöholm K, Palming J, Lystig TC, Jennische E, Woodruff TK, Carlsson B, Carlsson LM 2006 The expression of inhibin βB is high in human

adipocytes, reduced by weight loss, and correlates to factors implicated in metabolic disease. Biochem Biophys Res Commun 344:1308–1314
16. **Svensson PA, Gabrielsson BG, Jernås M, Gummesson A, Sjöholm K** 2008 Regulation of human aldoketoreductase 1C3 (AKR1C3) gene expression in the adipose tissue. Cell Mol Biol Lett 13:599–613
17. **Jernås M, Palming J, Sjöholm K, Jennische E, Svensson PA, Gabrielsson BG, Levin M, Sjögren A, Rudemo M, Lystig TC, Carlsson B, Carlsson LM, Lönn M** 2006 Separation of human adipocytes by size: hypertrophic fat cells display distinct gene expression. FASEB J 20: 1540–1542
18. **Gabrielsson BG, Johansson JM, Jennische E, Jernås M, Itoh Y, Peltonen M, Olbers T, Lönn L, Lönroth H, Sjöström L, Carlsson B, Carlsson LM, Lönn M** 2002 Depot-specific expression of fibroblast growth factors in human adipose tissue. Obes Res 10:608–616
19. **Chomczynski P, Sacchi N** 1987 Single-step method of RNA isolation by acid guanidinium thiocyanate-phenol-chloroform extraction. Anal Biochem 162:156–159
20. **Brazma A, Hingamp P, Quackenbush J, Sherlock G, Spellman P, Stoeckert C, Aach J, Ansorge W, Ball CA, Causton HC, Gaasterland T, Glenisson P, Holstege FC, Kim IF, Markowitz V, Matese JC, Parkinson H, Robinson A, Sarkans U, Schulze-Kremer S, Stewart J, Taylor R, Vilo J, Vingron M** 2001 Minimum information about a microarray experiment (MIAME)-toward standards for microarray data. Nat Genet 29:365–371
21. **Voros G, Maquoi E, Demeulemeester D, Clerx N, Collen D, Lijnen HR** 2005 Modulation of angiogenesis during adipose tissue development in murine models of obesity. Endocrinology 146:4545–4554
22. **Saiki A, Watanabe F, Murano T, Miyashita Y, Shirai K** 2006 Hepatocyte growth factor secreted by cultured adipocytes promotes tube formation of vascular endothelial cells in vitro. Int J Obes (Lond) 30:1676–1684
23. **Nishimura S, Manabe I, Nagasaki M, Hosoya Y, Yamashita H, Fujita H, Ohsugi M, Tobe K, Kadowaki T, Nagai R, Sugiura S** 2007 Adipogenesis in obesity requires close interplay between differentiating adipocytes, stromal cells, and blood vessels. Diabetes 56: 1517–1526

International Journal of Obesity (2006) 30, 1676–1684
 0307-0565/06 $30.00
www.nature.com/ijo

ORIGINAL ARTICLE

Hepatocyte growth factor secreted by cultured adipocytes promotes tube formation of vascular endothelial cells *in vitro*

A Saiki[1], F Watanabe[2], T Murano[2], Y Miyashita[1] and K Shirai[3]

[1]*Center of Diabetes, Endocrine and Metabolism, Sakura Hospital, School of Medicine, Toho University, Chiba, Japan;* [2]*Department of Clinical Laboratory, Sakura Hospital, School of Medicine, Toho University, Chiba, Japan and* [3]*Department of Internal Medicine, Sakura Hospital, School of Medicine, Toho University, Chiba, Japan*

Objective: Adipose tissue is closely associated with angiogenesis, but the mechanisms are not fully understood. Some of the adipocyte-derived cytokines are hypothesized to play an important role in angiogenesis. We evaluated tube formation of human umbilical vascular endothelial cells (HUVECs) cultured in type I collagen gel when overlaid with the supernatant of 3T3-L1 cell culture, and expression of tube-forming factor(s) in 3T3-L1 cells with or without pioglitazone. We also studied plasma growth factor levels in patients with type 2 diabetes mellitus treated with pioglitazone.

Results and methods: The supernatant of 3T3-L1 cells increased tube formation of HUVECs by 9.03-fold of control. Reverse transcription-polymerase chain reaction showed that hepatocyte growth factor (HGF) and vascular endothelial growth factor (VEGF) mRNA were expressed in 3T3-L1 cells. Western blot analysis also demonstrated HGF and VEGF protein expression. When 3T3-L1 cells were treated with 100 nM small interfering RNAs (siRNAs) for HGF, the HGF mRNA and protein were suppressed. The VEGF mRNA and protein in the cells were also suppressed by siRNA for VEGF. The supernatant of 3T3-L1 cells treated with HGF siRNA suppressed tube formation of HUVECs by 61% compared with the supernatant of cells treated with control siRNA. Addition of VEGF siRNA resulted in no significant changes. The supernatant conditioned with pioglitazone further promoted the tube formation. Pioglitazone enhanced HGF mRNA expression in 3T3-L1 cells. After 12 weeks of pioglitazone treatment, the changes of plasma HGF levels in patients treated with pioglitazone were significantly higher than those in control.

Conclusion: These results suggest that HGF secreted from 3T3-L1 cells may be the major factor regulating the tube formation, and agents that enhance the differentiation of adipocytes may promote tube formation of HUVECs mediated by HGF secreted by adipocytes.

International Journal of Obesity (2006) **30**, 1676–1684. doi:10.1038/sj.ijo.0803316; published online 21 March 2006

Keywords: angiogenesis; adipocyte; hepatocyte growth factor; pioglitazone; RNA interference

Introduction

Angiogenesis is the formation of new blood vessels by capillary sprouting from pre-existing vessels. Angiogenesis is a complex phenomenon, which includes proteolytic degradation of matrix, migration, proliferation and tube formation by vascular endothelial cells.[1] Especially, tube formation is recognized as a specific phenomenon for vascular endothelial cells, and it is possible to study the tube formation using vascular endothelial cells cultured in type 1 collagen gel.

Adipose tissue is closely associated with angiogenesis. Hausmann *et al.*[2] have reported differentiation of capillaries concurrent with adipogenesis in perivascular preadipocytes. Excessive growth of adipose tissue may require the formation of new capillaries for proper functioning.[3] However, the mechanisms by which adipose tissue induces angiogenesis are not fully understood. Adipose tissue is now recognized as an endocrine organ that secretes many cytokines and growth factors.[4,5] For example, several reports have demonstrated that adipocytes secrete tumor necrosis factor alpha,[6] resistin,[7] plasminogen activator inhibitor-1 (PAI-1),[8] leptin[9] and angiotensinogen.[10,11] Vascular endothelial growth factor (VEGF) is an angiogenetic growth factor, which is secreted by rat adipose tissue *ex vivo*.[12] Vascular endothelial growth

Correspondence: Dr Y Miyashita, Center of Diabetes, Endocrine and Metabolism, Sakura Hospital, School of Medicine, Toho University, 564-1, Shimoshizu, Sakura-City, Chiba 285-8741, Japan.
E-mail: mumon@sf6.so-net.ne.jp
Received 9 July 2005; revised 9 January 2006; accepted 12 February 2006; published online 21 March 2006

factor is considered to be the most potent and specific of the growth factors that regulate angiogenesis. Hepatocyte growth factor (HGF) is another endothelial growth factor with potent angiogenetic and mitogenic effects.[13,14] Recently, HGF as well as VEGF are being used in 'therapeutic angiogenesis'.[15,16] Serum HGF levels are elevated not only in patients with hepatic desease.[17] Rehman *et al.*[18] reported that levels of circulating HGF correlated with body mass index (BMI), and that HGF mRNA expression as measured by reverse transcription-polymerase chain reaction (RT-PCR) was increased in cultured adipocytes. However, the role of those cytokines secreted by adipocytes in tube formation of cultured vascular endothelial cells is not fully understood.

Some of the adipocyte-derived growth factors are hypothesized to promote tube formation of vascular endothelial cells. Therefore, we studied whether the factors secreted by 3T3-L1 cells induce tube formation of human umbilical venous endothelial cells (HUVECs) cultured in type 1 collagen gel. Next, we attempted to identify the tube-forming factor secreted by adipocytes by conducting RNA interference assays using small interfering RNAs (siRNAs)[19] targeting VEGF and HGF. Furthermore, we hypothesized that the increased presence of secretory adipose tissue would result in systemic elevations of VEGF and HGF. We also studied the plasma VEGF and HGF levels in patients with type 2 diabetes mellitus treated with pioglitazone, which was used to enhance differentiation of adipocytes.

Materials and methods

Human umbilical venous endothelial cell culture

Human umbilical venous endothelial cells were supplied by Cambrex Bio Science (Walkersville, Inc, Maryland, USA). The cells in endothelial cell basal medium (EBM; Cambrex, Co., East Rutherford) supplemented with 2.0% fetal calf serum (FCS) were seeded at a density of 2.0×10^4 cells in a 12-well plate. The medium was replaced once after 48 h. All experiments were performed on quiescent cells from the first passage.

In vitro *tube formation assay*

Eight volumes of type 1 collagen solution (Vitrogen 100; Collagen Corp., Santa Clara, CA, USA), 1 volume of 0.1 N NaOH and 1 volume of 10 × Dulbecco's modified Eagle's minimal essential medium (DMEM) were mixed on ice. A volume of 0.75 ml of the collagen mixture was dispensed into a well of a 12-well plate and allowed to gel at 37°C. 1×10^5 HUVECs in DMEM supplemented with 10% FCS were plated onto the collagen gel and cultured for 24 h at 37°C under 5% CO_2. Then, the medium was aspirated, and the cells were overlaid with 0.5 ml of the collagen mixture. After setting, 1.0 ml of DMEM containing the test factor was added. After 24 h incubation, the formation of capillary-like structure by HUVECs was observed.

Quantitative analysis of network structures

Phase-contrast photomicrographs (× 100 magnification) were recorded on a digital camera. The total length of the network structures was measured using the Scion Image software (Scion, Co., Washington, DC, USA). In all, 10 random fields were measured and the total length per field was calculated and expressed as a ratio to the control. In the control well, 1.0 ml of DMEM supplemented with 10% FCS was overlaid on the HUVEC culture in type 1 collagen mixture.

3T3-L1 cell culture

Mouse 3T3-L1 cells in DMEM supplemented with 10% FCS were cultured at 37°C under 5% CO_2. The cells (2.5×10^4 per well) were dispensed in a 12-well plate and incubated for 48 h. Then, the cells were incubated in the above-mentioned medium supplemented with dexamethasone (0.25 μM), 3-isobutyl-1-methyxanthine (0.5 mM) and insulin (10 μg/ml) for another 2 days. After incubation, the medium was replaced with DMEM containing 10% FCS with or without pioglitazone (endowed by Takeda Pharmaceutical Co., Ltd, Osaka) dissolved in dimethyl sulphoxide at a final concentration of 10 μM and incubated for 72 h. Pioglitazone was used to enhance differentiation of the 3T3-L1 cells. Then, the medium was replaced with DMEM supplemented with 10% FCS. After 24 h incubation, 1.0 ml of the supernatant was overlaid on type 1 collagen mixture containing HUVECs.

RNA interference of 3T3-L1 cells

To identify the angiogenetic factor secreted from 3T3-L1 cells, we performed RNA interference assays on 3T3-L1 cells using siRNAs (Ambion, Inc., Austin, TX, USA). Murine HGF siRNAs targeting the sense sequence 5′-GGU GGA GAA GAG AGC Utt-3′ and the antisense sequence 5′-AGC UCU CUU CUU CUC CAC Ctg-3′ were selected. Murine VEGF siRNAs targeting the sense sequence 5′-GGA GAG CAG AAG UCC CAU Gtt-3′ and the antisense sequence 5′-CAU GGG ACU UCU GCU CUC Ctt-3′ were also selected. Silencer™ (Ambion, Inc.) siRNA was used as the negative control. Mouse 3T3-L1 cells were cultured in DMEM with 10% FCS for 48 h, then the cells were incubated in the above-mentioned medium with dexamethasone, 3-isobutyl-1-methyxanthine and insulin for another 2 days. The siPORT™ *amine* (Ambion, Inc.) was diluted in serum-free minimum essential medium and kept at room temperature for 30 min. Then, 5 or 10 μl of 20 μM siRNA (final concentration 50 or 100 nM for murine HGF or VEGF (Ambion, Inc.) was added to the diluted siPORT™ amine transfection agent and left at room temperature for 15 min. After adjustment the volume of normal DMEM in each well containing cells to 400 and 100 μl of the transfection agent/siRNA mixture was added and incubated at 37°C for 24 h. Then, 2 ml of fresh medium was added to each well and the cells were incubated for 24 h. After incubation, the supernatant and cells were used for studies.

Reverse transcription-polymerase chain reaction of hepatocyte growth factor or vascular endothelial growth factor mRNA in 3T3-L1 cells

Total RNA was isolated from 3T3-L1 cells grown in a six-well plate using RNeasy® Mini Kit (QIAGEN GmbH, Hilden, Germany). The amount of RNA was measured as the absorbance at 260 nm. Synthesis of complementary DNA (cDNA) and PCR were performed using the RNA PCR Kit (AMV) Ver.3.0 (Takara, Ohtsu, Japan). A pair of gene-specific PCR primers each was designed for HGF and VEGF. The following primer sets were used: HGF forward primer, 5′-CCATgAATTTgACCTCTATgA-3′; HGF reverse primer, 5′-CTgAggAATCTCACAgACTTC-3′. VEGF forward primer, 5′-TgAACTTTCTgCTCTCTTgg-3′; VEGF reverse primer, 5′-AACAAATgCTTTCTCCgCTC-3′; First-strand cDNA was synthesized from 1 μg of total RNA. Total RNA was mixed with 0.25 U of reverse transcriptase, 1 mM of deoxynucleoside triphosphate mixture, 2.5 μM of first-strand cDNA primer (random 9 mers; Takara, Ohtsu, Japan), 0.25 U of RNase inhibitor and 6 μl of $MgCl_2$ reaction buffer in a final volume of 10 μl and incubated at 30°C for 10 min, followed by 30 min at 42°C, 5 min at 99°C and 5 min at 5°C. The PCR mixture contained 0.4 μM of each primer, 0.25 μl of Takara Ex Taq HS™ as DNA polymerase and 5.0 mM of $MgCl_2$ reaction buffer in a final volume of 40 μl for synthesizing the second-strand cDNA. Amplification was performed for 30 cycles under the following conditions: denaturation at 95°C for 5 min for the first cycle and 30 s for subsequent cycles, annealing at 55°C for 30 s and extension at 72°C for 90 s. The PCR products were separated by electrophoresis on a 3.0% agarose gel, and then visualized by staining with 1 mg/ml ethidium bromide. The quantities of reaction products were determined using digital scanning and Scion Image software.

Western blot analysis of hepatocyte growth factor or vascular endothelial growth factor protein in 3T3-L1 cells

Hepatocyte growth factor and/or VEGF protein expression in 3T3-L1 cells was detected by Western blot analysis. Cells were suspended in a lysis buffer containing 10 mM Tris-HCl (pH 7.5), 150 mM NaCl, 0.5% Triton X-100, 0.5 mM phenylmethylsulfonyl fluoride and 1 mM ethylenediamine tetraacetate (EDTA) for 4 h at 4°C. After centrifugation at 12 000 *g*, the protein concentration in the supernatant was measured using the Bio-Rad protein assay. Samples were diluted 1:1 with electrophoresis sample buffer containing 100 mM Tris (pH 6.8), 10% sodium dodecyl sulfate (SDS), 10% glycerol, 0.1% bromophenol blue and 5% β-mercaptoethanol. They were boiled for 5 min and electrophoresed on 10% SDS-polyacrylamide gel. The proteins were transferred onto Hybond-ECL nitrocellulose membrane (Amersham, Piscataway, NJ, USA). After blotting, the membrane was washed with Tris buffer saline (TBS; 100 mM Tris, pH 7.5, 0.9% NaCl) and blocked with 5% bovine serum albumin in TBS, followed by a brief wash in TBS containing 0.1% Tween-20 (TTBS) and incubation with antiserum against murine HGF (Santa Cruz Biotechnology, Inc., CA, USA) and murine VEGF (TECNE corporation, Minneapolis, MN, USA) at a dilution of 1:500 for 2 h at room temperature. After washing with TTBS, the blot was incubated with peroxidase-labeled affinity-purified antibody to chicken immunoglobulin-G (H + L) (KPL, UK) at a dilution of 1:1500 for 1 h at room temperature, washed with TTBS and incubated with 1:3000 diluted biotinylated HP streptavidin complex for 1 h at a room temperature. The antigen–antibody complex was visualized by photo detection. The reaction products were quantified using digital scanning and Scion Image software.

Subjects

The randomized, open study was performed at the Center of Diabetes, Endocrinology and Metabolism, Sakura Hospital, School of Medicine, Toho University. A total of 50 Japanese subjects (29 males and 21 females) with type 2 diabetes mellitus, who had not been treated with pioglitazone, were eligible for enrollment. Patients with cancer, myocardial infarction, cerebral infarction and arteriosclerosis obliterans were excluded from this study. Before administration of pioglitazone, 34 patients had been treated with sulfonylureas and 16 had been treated with diet alone. The same dose of sulfonylureas had been continued during pioglitazone administration. The patients were randomly divided into two groups. One group was administered pioglitazone 30 mg/day (pioglitazone group, $n=25$) and the other group was not administered (control group, $n=25$) for 12 weeks. Clinical characteristics of this study subject are shown in Table 1. Dietary counseling was undertaken by a dietary assistant and patients were asked to avoid any changes in diet or lifestyle for the duration of the study. The study was approved by the institutional review board and all patients provided written informed consent before participation in the study.

Measurement of plasma hepatocyte growth factor and vascular endothelial growth factor

Blood samples were withdrawn in the morning after 12 h of fasting. The samples were collected in tubes containing di-sodium EDTA, centrifuged at 3000 *g* for 10 min at 4°C and frozen at −80°C. Plasma HGF levels were determined by using enzyme-linked immunosorbent assay (ELISA) kits (HGF Otsuka ELISA kit, Otsuka, Tokyo) and plasma VEGF levels were determined by using ELISA kits (human VEGF Quantikine, R&D Systems, Minneapolis, MN, USA).

Statistical analysis

Stat View-J 5.0 software was used for all statistical analysis. Paired *t*-test was carried out to determine if the differences between groups were statistically significant. $P<0.05$ was considered to be significant.

Table 1 Baseline characteristics of 50 patients with type 2 diabetes mellitus

	Pioglitazone (n = 25)	*Control (n = 25)*	*P-value*
Age (years)	63.8±12.6	61.4±12.3	NS
Male/female	15/10	14/11	–
Height (m)	159.9±6.6	161.2±7.9	NS
Weight (kg)	61.4±7.7	61.6±12.8	NS
BMI (kg/m^2)	24.0±2.5	23.6±3.6	NS
Systolic blood pressure (mm Hg)	131.9±12.7	133.4±12.2	NS
Diastolic blood pressure (mm Hg)	75.0±9.2	78.1±7.2	NS
Asparate aminotransferase (IU/l)	31.2±19.9	26.9±13.0	NS
Alanine aminotransferase (IU/l)	29.0±23.2	27.8±16.6	NS
γ-Glutamyl transpeptidase (IU/1)	48.9±39.0	43.2±32.9	NS
Serum creatinine (μmol/l)	72.1±31.8	67.1±20.2	NS
Fasting blood glucose (mmol/l)	9.73±4.63	9.76±3.69	NS
HbA_{1c} (%)	8.17±0.87	7.95±0.87	NS
Total cholesterol (mmol/l)	5.12±1.02	5.30±0.98	NS
Triglyceride (mmol/l)	1.42±0.84	1.45±0.92	NS
High-density lipoprotein cholesterol (mmol/l)	1.41±0.45	1.42±0.38	NS
Low-density lipoprotein cholesterol (mmol/l)	3.01±0.80	3.10±0.85	NS
HGF (ng/ml)	0.256±0.044	0.259±0.079	NS
VEGF (pg/ml)	262.0±188.6	261.7±254.5	NS

Values are expressed as mean±s.d. Abbreviations: HGF, hepatocyte growth factor; NS, not significant; VEGF, vascular endothelial growth factor.

Results

In vitro *tube formation induced by supernatant of 3T3-L1 cells*
To evaluate whether the adipocyte-derived growth factors promote tube formation of vascular endothelial cells *in vitro*, the supernatant of the 3T3-L1 cells was overlaid on type 1 collagen mixture containing HUVECs (Figure 1). The supernatant of the 3T3-L1 cells treated with dexamethasone, 3-isobutyl-1-methyxanthine and insulin dramatically induced tube formation compared with control (9.03-fold increase). The supernatant conditioned with pioglitazone after induction of adipocyte differentiation further promoted the tube formation compared with control (12.36-fold increase). Growth medium with 10 μM pioglitazone did not induce tube formation. These results suggested that 3T3-L1 cells secreted some tube-forming factors, and these factors might be increased with differentiation of the adipocytes.

Hepatocyte growth factor and/or vascular endothelial growth factor mRNA expression in 3T3-L1 cells
To identify the tube-forming factor(s) secreted by 3T3-L1 cells, HGF and VEGF mRNA in the cells were studied as candidates (Figure 2). Expression of HGF and VEGF mRNA in 3T3-L1 cells was demonstrated by RT-PCR. Strong HGF mRNA expression and VEGF mRNA expression in 3T3-L1 cells were detected by RT-PCR. Both HGF and VEGF mRNA expression in 3T3-L1 cells were suppressed by treatment with siRNAs for HGF and VEGF, respectively. These results indicated that 3T3-L1 cells expressed growth factors, notably HGF and VEGF. Furthermore, the data confirmed that siRNA for HGF and VEGF effectively interfered with the mRNA expression.

Hepatocyte growth factor and/or vascular endothelial growth factor protein expression in 3T3-L1 cells
Expression of HGF and VEGF protein in 3T3-L1 cells was demonstrated by Western blot analysis (Figure 3). Both HGF and VEGF protein expressions in 3T3-L1 cells were detected by RT-PCR and they were suppressed by treatment with siRNAs for HGF and VEGF, respectively, as well as those mRNA expressions detected by RT-PCR.

Tube formation by supernatant of 3T3-L1 cells treated with small interfering RNA
While the data confirmed that 3T3-L1 cells express HGF and VEGF, it remains unclear whether HGF and VEGF are actually potent tube-forming factor secreted from adipocytes. To identify the tube formation-inducing factor, we studied whether the supernatant of 3T3-L1 cells treated with siRNAs for HGF or VEGF suppresses the tube formation *in vitro* (Figure 4). Addition of control siRNA (100 nM) did not suppress the increase in tube formation induced by the supernatant of 3T3-L1 cells. The supernatant of adipocytes treated with siRNA for VEGF also did not suppress the tube formation compared with the addition of control siRNA. The supernatant of adipocytes treated with 50 or 100 nM of siRNA for HGF suppressed the tube formation compared with the addition of control siRNA. The siRNA for HGF (100 nM) suppressed the *in vitro* tube formation by 61% compared with the control siRNA.

Hepatocyte growth factor and/or vascular growth factor mRNA expression in 3T3-L1 cells conditioned with pioglitazone
Figure 1 shows that the supernatant of differentiated 3T3-L1 cells conditioned with pioglitazone further promoted the

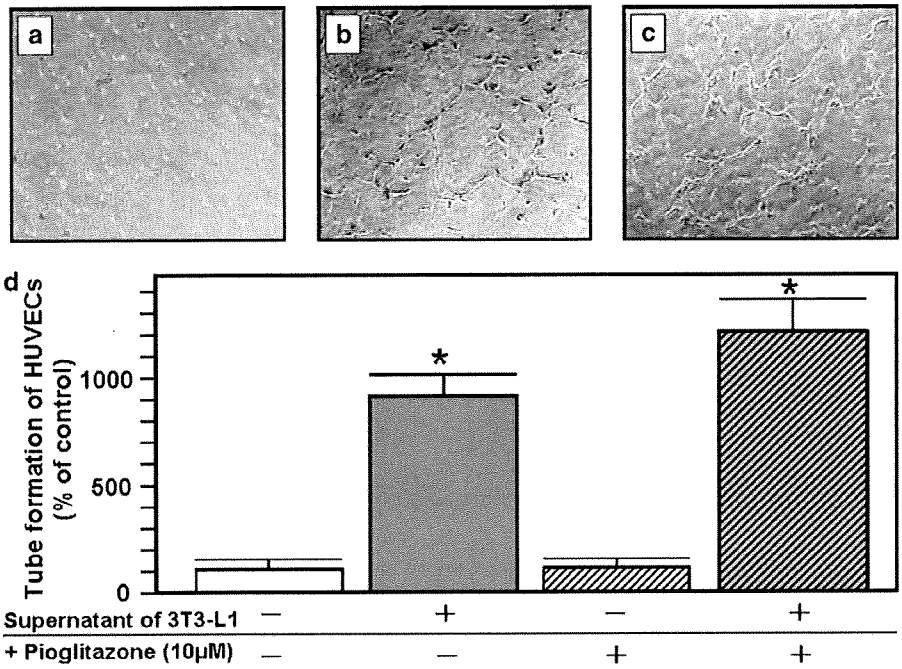

Figure 1 *In vitro* tube formation stimulated by supernatant of 3T3-L1 cells. After 1.0 ml of the supernatant of 3T3-L1 cells was treated by dexamethasone, 3-isobutyl-1-methyxanthine and insulin or medium was added into the type 1 collagen mixture containing human umbilical vascular endothelial cells (HUVECs), and phase-contrast photomicrographs (× 100 magnification) were recorded on a digital camera. (**a**) Control: growth medium. (**b**) Supernatant of 3T3-L1 cells. (**c**) Supernatant of 3T3-L1 cells treated with 10 μM of pioglitazone. (**d**) Quantitative analysis of network structures. Total length of the network structures was measured and total length per field was calculated and expressed as a ratio to control. Values are expressed in mean ± s.d. *$P<0.001$ compared with control.

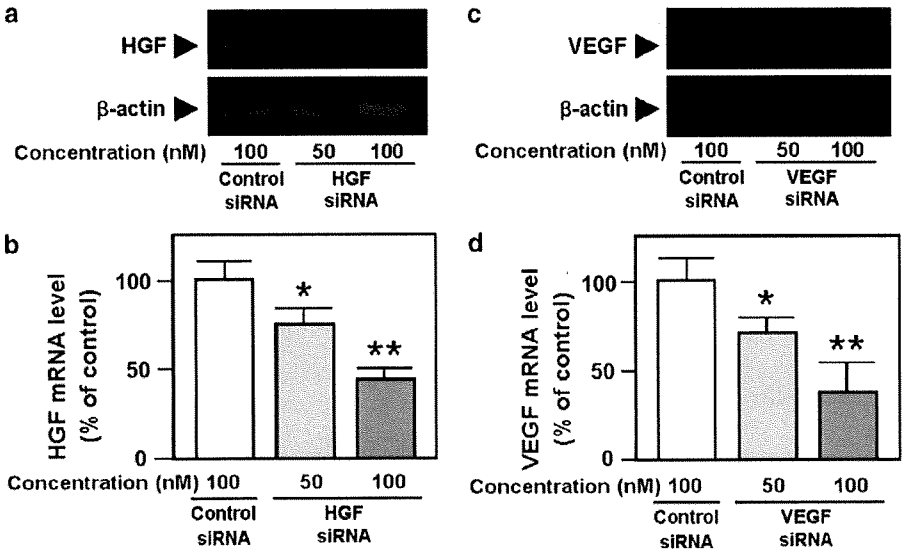

Figure 2 Hepatocytic growth factor (HGF) and vascular endothelial growth factor (VEGF) mRNA expression in 3T3-L1 cells. Hepatocytic growth factor and VEGF mRNA in 3T3-L1 cells treated with dexamethasone, 3-isobutyl-1-methyxanthine and insulin was detected by reverse transcription-polymerase chain reaction (RT-PCR). (**a**) Hepatocytic growth factor mRNA expression in 3T3-L1 cells detected by RT-PCR using a pair of gene-specific PCR primers designed for HGF. Far left lane: HGF mRNA expression in the cells treated with 100 nM of control small interfering RNA (siRNA); lanes 2 and 3 from the left: HGF mRNA expression in the cells treated with 50 and 100 nM of HGF siRNA, respectively. (**b**) Quantitative analysis of HGF mRNA expression in the cells treated with control siRNA or HGF siRNA. (**c**) Vascular endothelial growth factor mRNA expression in the cells detected by RT-PCR using a pair of gene-specific PCR primers designed for VEGF. Far left lane: VEGF mRNA expression in the cells treated with 100 nM of control siRNA; lanes 2 and 3 from the left: VEGF mRNA expression in the cells treated with 50 and 100 nM of VEGF siRNA, respectively. (**d**) Quantitative analysis of VEGF mRNA expression in the cells treated with control siRNA or VEGF siRNA. The products were quantified by digital scanning and Scion Image software. Values are expressed in mean ± s.d. *$P<0.05$, and **$P<0.005$ compared with control.

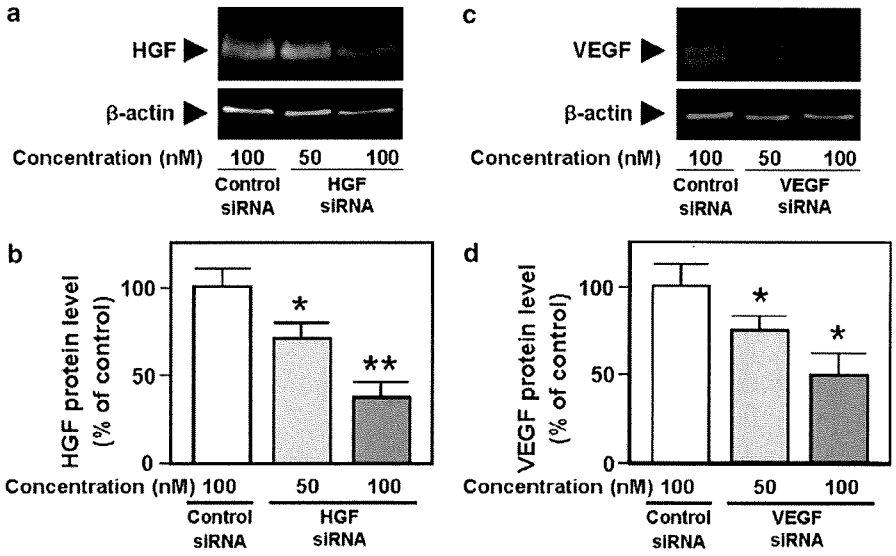

Figure 3 Hepatocytic growth factor (HGF) and vascular endothelial growth factor (VEGF) protein expression in 3T3-L1 cells. Hepatocytic growth factor or VEGF protein in 3T3-L1 cells treated by dexamethasone, 3-isobutyl-1-methyxanthine and insulin was detected by Western blot analysis. (**a**) Hepatocytic growth factor protein expression in the cells was detected by anti-murine HGF antibody. Far left lane: HGF protein expression in the cells treated with 100 nM of control small interfering RNA (siRNA); lanes 2 and 3 from the left: HGF protein expression in the cells treated with 50 and 100 nM of HGF siRNA, respectively. (**b**) Quantitative analysis of HGF protein expression in the cells treated with control siRNA or HGF siRNA. (**c**) Vascular endothelial growth factor protein expression in the cells was detected by Western blot analysis using anti-murine VEGF antibody. Far left lane: VEGF protein expression in the cells treated with 100 nM of control siRNA; lanes 2 and 3 from the left: VEGF protein expression in the cells treated with 50 and 100 nM of VEGF siRNA, respectively. (**d**) Quantitative analysis of VEGF protein expression in the cells treated with control siRNA or VEGF siRNA. The products were quantified by digital scanning and Scion Image software. Values are expressed in mean ± s.d. $^{*}P<0.05$ and $^{**}P<0.005$ compared with control.

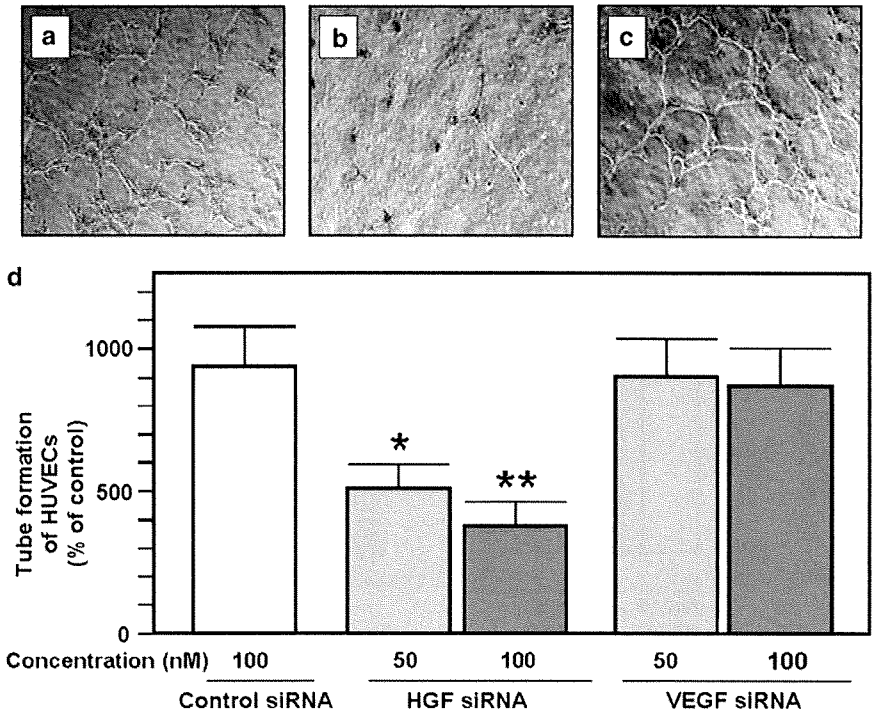

Figure 4 Effect of the supernatants of differentiated 3T3-L1 cells treated with small interfering RNAs (siRNAs) for hepatocytic growth factor (HGF) and vascular endothelial growth factor (VEGF) on tube formation *in vitro*. Phase-contrast photomicrographs (× 100 magnification) were recorded on a digital camera. (**a**) Supernatant of 3T3-L1 cells treated with 100 nM of control siRNA was added onto type 1 collagen mixture containing human umbilical vascular endothelial cells (HUVECs). (**b**) Supernatant of the cells treated with 100 nM of HGF siRNA was added. (**c**) Supernatant of the cells treated with 100 nM of VEGF siRNA was added. (**d**) Quantitative analysis of tube formation of HUVECs overlaid with supernatant of 3T3-L1 cells treated with control siRNA, HGF siRNA or VEGF siRNA. Values are expressed as mean ± s.d. $^{*}P<0.05$ and $^{**}P<0.005$ compared with control.

tube formation compared with the supernatant of the cells conditioned without pioglitazone. To clarify the tube-forming factor(s) in 3T3-L1 cells enhanced by addition of pioglitazone, expressions of HGF and VEGF mRNA in the cells that were conditioned with pioglitazone were demonstrated by RT-PCR (Figure 5). Reverse transcription-polymerase chain reaction showed that HGF mRNA expression in 3T3-L1 cells conditioned with pioglitazone was enhanced by 33% compared with that in the cells conditioned without pioglitazone. On the other hand, VEGF mRNA expression in the cells was not enhanced when the cells were conditioned with pioglitazone.

Effects of pioglitazone on plasma hepatocyte growth factor and vascular endothelial growth factor levels in patients with type 2 diabetes mellitus

As shown in Figure 6, the changes of BMI and HbA_{1C} in the pioglitazone group were significantly higher than those in the control group. The change of plasma HGF levels in the pioglitazone group was also significantly higher than those in the control group ($P=0.0479$), whereas no significant differences in the change of plasma VEGF levels were observed between the pioglitazone group and the control group. In the pioglitazone group, the change of plasma HGF levels showed a positive correlation with the change of BMI

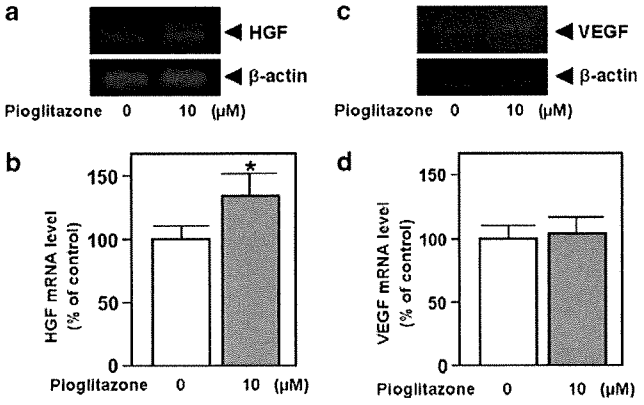

Figure 5 Hepatocytic growth factor (HGF) and vascular endothelial growth factor (VEGF) mRNA expression in 3T3-L1 cells treated with pioglitazone. The cells treated with 10 μM of pioglitazone after induction of differentiation. Hepatocytic growth factor and VEGF mRNA in the cells was detected by reverse transcription-polymerase chain reaction (RT-PCR). (**a**) HGF mRNA expression in the cells detected by RT-PCR using a pair of gene-specific PCR primers designed for HGF. Far left lane: HGF mRNA expression in the cells (control); lane 2 from the left: HGF mRNA expression of cells treated with 10 μM of pioglitazone. (**b**) Quantitative analysis of HGF mRNA expression in the cells treated with 10 μM of pioglitazone. (**c**) Vascular endothelial growth factor mRNA expression in the cells detected by RT-PCR using a pair of gene-specific PCR primers designed for VEGF. Far left lane: VEGF mRNA expression in the cells (control); lane 2 from the left: VEGF mRNA expression of cells treated with 10 μM of pioglitazone. (**d**) Quantitative analysis of VEGF mRNA expression in the cells treated with 10 μM of pioglitazone. The products were quantified by digital scanning and Scion Image software. Values are expressed in mean $\pm$ s.d. *$P<0.05$ compared with control.

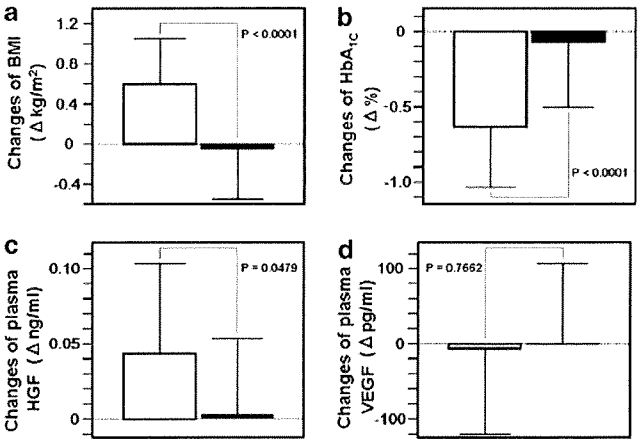

Figure 6 The changes of body mass index (BMI) (**a**), HbA_{1C} (**b**), plasma HGF (**c**) and plasma VEGF (**d**) in 50 subjects randomized to receive either 30 mg pioglitazone orally once daily ($n=25$, white bars) or control ($n=25$, black bars) for 12 weeks. The data are shown as mean $\pm$ s.d.

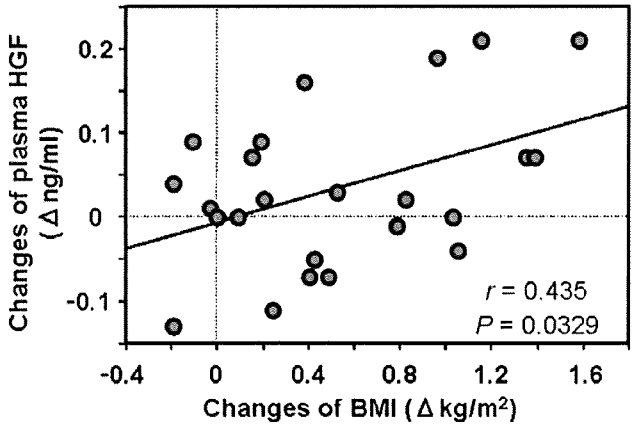

Figure 7 Correlation between change of body mass index (BMI) and change of plasma hepatocytic growth factor (plasma HGF). Increase in BMI and increase in plasma HGF show a significant correlation ($r=0.435$, $P=0.0329$).

($r=0.435$, $P=0.0329$) (Figure 7). However, the change of plasma HGF levels did not show correlation with asparate aminotransferase, alanine aminotransferase, γ-glutamyl transpeptidase, fasting blood glucose, HbA_{1C} and plasma lipid levels in the group (data not shown).

Discussion

In this study, the supernatant of 3T3-L1 cells, which were induced of differentiation by dexamethasone, 3-isobutyl-1-

methyxanthine and insulin, strongly promoted tube formation of HUVECs cultured in type 1 collagen gel. Reverse transcription-polymerase chain reaction showed that 3T3-L1 cells expressed both HGF and VEGF mRNA. Western blot analysis also demonstrated both HGF and VEGF protein. The supernatant of 3T3-L1 cells treated with siRNA for HGF suppressed the tube formation of HUVECs compared with control siRNA, whereas the supernatant of the cells treated with siRNA for VEGF did not suppress. These results indicate that VEGF may also contribute in part to promote tube formation by adipocytes. However, our results suggest that HGF is the major angiogenetic factor secreted by adipocytes, because the supernatant of differentiated 3T3-L1 cells treated with siRNA for HGF failed to promote tube formation. Although HGF has been reported to be secreted by mature adipocytes,[18] no report has shown that the HGF secreted by mature adipocytes is associated with angiogenesis. Our report provides the first evidence that HGF secreted by adipocytes promotes tube formation of HUVECs.

Several studies have reported that adipocytes secrete angiogenetic factors. Claffey *et al.*[20] reported that VEGF expression was regulated by differentiation of 3T3-L1 cells. *In vivo*, Silha *et al.*[21] reported that serum concentrations of VEGF were significantly elevated in human overweight and obese subjects. Matrix metalloproteases are produced by human adipose tissue,[22] and are expressed in adipose tissue during obesity and modulate adipocyte differentiation.[23-] Dobson *et al.*[24] reported that 1-butyryl-glycerol was secreted by adipocytes, and that synthetic 1-butyryl-glycerol stimulated angiogenesis *in vivo* and *in vitro*. Leptin has also been reported to enhance tube formation *in vitro*.[25] A limitation of this study is that the findings are limited to demonstrating only about the HGF and the VEGF. In future studies, we should confirm whether those angiogenetic factor expressions in 3T3-L1 cells are shown and whether the supernatant of the cells treated with siRNAs for those factors suppress the tube formation of HUVECs. Also, the abnormalities of the VEGF receptor signaling pathway of the HUVECs might present under the conditions of this study. At least, the supernatant of 3T3-L1 cells did not suppress expressions of VEGF receptor 1 and 2 protein in HUVECs by Western blot analysis using phospho-specific antibodies to the VEGF receptor 1 and 2 compared with DMEM supplemented with 10% FCS (data not shown).

Pioglitazone is one of the thiazolidinediones that activate the peroxisome proliferator-activated receptor γ (PPARγ), which is expressed primarily in adipose tissue. Forced expression of PPARγ in the fibroblasts makes them differentiate into adipocytes.[26] The supernatant of the cells, differentiation in which was enhanced by addition of pioglitazone, potently promoted the tube formation of HUVECs. The enhancement of HGF mRNA expression in 3T3-L1 cells conditioned with pioglitazone was demonstrated by RT-PCR. Furthermore, plasma HGF levels increased in patients with type 2 diabetes mellitus after treatment with pioglitazone, and the change of plasma HGF levels showed a positive correlation with the change of BMI in the pioglitazone group. These results supported that the differentiation of adipocytes might enhance the HGF expression *in vitro* and *in vivo*. However, currently, the mechanism by which pioglitazone activates the HGF expression in adipocytes is not fully understood.

Hepatocyte growth factor was purified from rat platelets and characterized as a growth factor for mature parenchymal hepatocytes.[27] Several recent studies have reported that HGF exhibits angiogenetic actions. Morishita *et al.*[28] reported that treatment with human recombinant HGF improved hindlimb ischemia in rabbits. Human recombinant HGF has been applied in therapeutic angiogenesis, as a cytokine supplement for patients with arteriosclerosis obliterans.[29] Hepatocyte growth factor is also seen as a significant cardioprotective factor because of its potent angiogenetic properties[14,30] and because HGF can reduce restenosis after balloon injury by enhancing re-endothelialization.[31] On the other hand, plasma HGF levels are elevated in malignancies,[32] patients with atherosclerosis and proliferative diabetic retinopathy.[33,34] The findings indicate that obesity might affect processes such as tumor angiogenesis or proliferative diabetic retinopathy mediated by HGF. Future studies should investigate whether specific inhibitors or modulators of HGF production and signaling pathways might indeed serve as targets for vascular therapies.

In summary, the supernatant of differentiated 3T3-L1 cells strongly promotes tube formation of HUVECs cultured in type 1 collagen gel, and HGF secreted from 3T3-L1 cells may be the major factor regulating the tube formation. The supernatant supplemented with pioglitazone further enhances the tube formation. Pioglitazone enhanced HGF mRNA expression in 3T3-L1 cells and increased plasma HGF levels in patients with type 2 diabetes mellitus. These results suggest that agents that enhance the differentiation of adipocytes may promote tube formation of HUVECs mediated by HGF secreted by adipocytes.

References

1 Folkman J. How is blood vessel growth regulated in normal and neoplastic tissue? G.H.A. Clowes memorial Award lecture. *Cancer Res* 1986; **46**: 467–473.
2 Hausman GJ, Richardson LR. Histochemical and ultrastructural analysis of developing adipocytes in the fetal pig. *Acta Anat* 1982; **114**: 228–247.
3 Crandall DL, Hausman GJ, Kral JG. A review of the microcirculation of adipose tissue: anatomic, metabolic, and angiogenic perspectives. *Microcirculation* 1997; **4**: 211–232.
4 Coppack SW. Pro-inflammatory cytokines and adipose tissue. *Proc Nutr Soc* 2001; **60**: 349–356.
5 Trayhurn P, Beattie JH. Physiological role of adipose tissue: white adipose tissue as an endocrine and secretary organ. *Proc Nutr Soc* 2001; **60**: 329–339.
6 Hotamisligil GS, Shargill NS, Spiegelman BM. Adipose expression of tumor necrosis factor-alpha: direct role in obesity-linked insulin resistance. *Science* 1993; **259**: 87–91.

7 Yamauchi T, Kamon J, Waki H, Murakami K, Motojima K, Komeda K *et al.* The mechanisms by which both heterozygous peroxisome proliferator-activated receptor gamma (PPAR gamma) deficiency and PPAR gamma agonist improve insulin resistance. *J Biol Chem* 2001; **276**: 41245–41254.
8 Skurk T, Hauner H. Obesity and impaired fibrinolysis: role of adipose production of plasminogen activator inhibitor-1. *Int Obes Relat Metab Disord* 2004; **28**: 1357–1364.
9 Caro J, Sinha M, Kolaczynski J, Zhang P, Considine R. Leptin: the tale of an obesity gene. *Diabetes* 1996; **45**: 1445–1462.
10 Sharma A, Janke J, Gorzeliniak K, Engeli S, Luft C. Angiotensin blockade prevents type 2 diabetes by formation of fat cells. *Hypertension* 2002; **40**: 609–622.
11 Gorzeliniak K, Engeli S, Janke J, Luft C, Sharma A. Hormonal regulation of the human adipose-tissue rennin–angiotensin system: relationship to obesity and hypertension. *J Hypertens* 2002; **20**: 965–973.
12 Mick GJ, Wang X, McCormick K. White adipocyte vascular endothelial growth factor: regulation by insulin. *Endocrinology* 2002; **143**: 948–953.
13 Nakagami H, Morishita R, Yamamoto K, Taniyama Y, Aoki M, Matsumoto K *et al.* Mitogenic and antiapoptotic actions of hepatocyte growth factor through ERK, STAT3, and AKT in endothelial cells. *Hypertension* 2001; **37**: 581–586.
14 Morishita R, Sakaki M, Yamamoto K, Iguchi S, Aoki M, Yamasaki K *et al.* Impairment of collateral formation in lipoprotein(a) transgenic mice: therapeutic angiogenesis induced by human hepatocyte growth factor gene. *Circulation* 2002; **105**: 1491–1496.
15 Hockel M, Schlenger K, Doctrow S, Kissel T, Vaupel P. Therapeutic angiogenesis. *Arch Surg* 1993; **128**: 423–429.
16 Funatsu T, Sawa Y, Ohtake S, Takahashi T, Matsumiya G, Matsuura N *et al.* Therapeutic angiogenesis in the ischemic canine heart induced by myocardial injection of naked complementary DNA plasmid encoding hepatocyte growth factor. *J Thorac Cardiovasc Surg* 2002; **124**: 1099–1105.
17 Shiota G, Umeki K, Okano J, Kawasaki H. Hepatocyte growth factor and acute phase proteins in patients with chronic liver diseases. *J Med* 1995; **26**: 295–308.
18 Rehman J, Considine R, Bovenkerk J, Li J, Slavens C, Jones R *et al.* Obesity is associated with increased levels of circulating hepatocyte growth factor. *J Am Coll Cardiol* 2003; **41**: 1408–1413.
19 Elbashir SM, Lendeckel W, Tuschi T. RNA interference is mediated by 21- and 22-nucleotide RNAs. *Genes Dev* 2001; **15**: 188–200.
20 Claffey KP, Wilkison WO, Spiegelman BM. Vascular endothelial growth factor. Regulation by cell differentiation and activated second messenger pathways. *J Biol Chem* 1992; **267**: 16317–16322.
21 Silha JV, Krsek M, Sucharda P, Murphy LJ. Angiogenic factors are elevated in overweight and obese individuals. *Int J Obes Relat Metab Disord* 2005; **29**: 1308–1314.
22 Bouloumie A, Sengines C, Portalan G, Galitzky J, Lafontan M. Adipocyte produces matrix metalloproteinases 2 and 9 involvement in adipose differentiation. *Diabetes* 2001; **50**: 2080–2086.
23 Chavey C, Mari B, Mounthouel M, Bonnafous S, Anglard P, Obberghen E *et al.* Matrix metalloproteinases are differentially expressed in adipose tissue during obesity and modulate adipocyte differentiation. *J Biol Chem* 2003; **278**: 11888–11896.
24 Dobson D, Kambe A, Block E, Dion T, Lu H, Castellot J *et al.* 1-Butyryl-glycerol: a novel angiogenesis factor secreted by differentiating adipocytes. *Cell* 1990; **61**: 223–230.
25 Bouloumie A, Drexler H, Lafontan M, Busse R. Leptin, the product of gene, promotes angiogenesis. *Circ Res* 1998; **83**: 1059–1066.
26 Tontonoz P, Hu E, Spiegelman BM. Stimulation of adipogenesis in fibroblasts by PPAR gamma 2, a lipid-activated transcription factor. *Cell* 1994; **79**: 1147–1156.
27 Nakamura T, Teramoto H, Ichihara A. Purification and characterization of a growth factor from rat platelets for mature parenchymal hepatocytes in primary cultures. *Proc Natl Acad Sci USA* 1986; **83**: 6489–6493.
28 Morishita R, Nakamura S, Hayashi S, Taniyama Y, Moriguchi A, Nagano T *et al.* Therapeutic angiogenesis induced by human recombinant hepatocyte growth factor in rabbit hind limb ischemia model as cytokine supplement therapy. *Hypertension* 1999; **33**: 1379–1384.
29 Aoki M, Morishita R, Taniyama Y, Kaneda Y, Ogihara T. Therapeutic angiogenesis induced by hepatocyte growth factor: potential gene therapy for ischemic disease. *J Atheroscler Thomb* 2000; **7**: 71–76.
30 Taniyama Y, Morishita R, Hiraoka K, Aoki M, Nakagami H, Yamasaki K *et al.* Therapeutic angiogenesis induced by human hepatocyte growth factor gene in rat diabetic hind limb ischemia model: molecular mechanisms of delayed angiogenesis in diabetes. *Circulation* 2001; **104**: 2344–2350.
31 Yasuda S, Noguchi T, Gohda M, Arai T, Tsutsui N, Matsuda T *et al.* Single low-dose administration of human recombinant hepatocyte growth factor attenuates intimal hyperplasia in a balloon-injured rabbit iliac artery model. *Circulation* 2000; **101**: 2546–2549.
32 Seidel C, Borset M, Turesson I, Abildgaard N, Sundan A, Waage A. Elevated serum concentrations of hepatocyte growth factor in patients with multiple myeloma. The Nordic Myeloma Study Group. *Blood* 1998; **91**: 806–812.
33 Nishimura M, Nakano K, Ushiyama M, Nanbu A, Ohtsuka K, Takahashi H *et al.* Increased serum concentrations of human hepatocyte growth factor in proliferative diabetic retinopathy. *J Clin Endocrinol Metab* 1998; **83**: 195–198.
34 Tateishi J, Waku S, Masutani M, Ohyanagi M, Iwasaki T. Hepatocyte growth factor as a potential predictor of the presence of atherosclerotic aorto-iliac artery disease. *Am Heart J* 2002; **143**: 272–276.